



Research Article

Martina F. Ober, Adrian Müller-Deku, Anna Baptist, Benjamin Ajanović, Heinz Amenitsch, Oliver Thorn-Seshold and Bert Nickel*

SAXS measurements of azobenzene lipid vesicles reveal buffer-dependent photoswitching and quantitative $Z \rightarrow E$ isomerisation by X-rays

<https://doi.org/10.1515/nanoph-2022-0053>

Received February 3, 2022; accepted April 3, 2022;

published online April 15, 2022

Abstract: Photoresponsive materials feature properties that can be adjusted by light near-instantaneously, reversibly, and with high spatiotemporal precision. There is considerable interest in maximising the degree of photoswitching, and in measuring this degree during illumination in complex environments. We study the switching of photoresponsive lipid membranes that allow for precise and reversible manipulation of membrane shape, permeability, and fluidity. Though these macroscopic responses are clear, it is unclear how large the changes of *trans/cis* ratio are, and whether they can be improved. Here, we used small-angle X-ray scattering to measure the thickness of photoswitchable lipid membranes, and we correlate lipid bilayer thickness to *trans/cis* ratios. This reveals an unexpected dependency of photoswitching ratio upon aqueous phase composition. In buffer with ionic strength, we observe thickness variations twice as large as previously observed. Furthermore, soft X-rays can quantitatively isomerise photolipid membranes to the all-*trans* state;

enabling X-ray-based membrane control. High energy X-rays do not influence the state of the photoswitches, presumably because they deposit less dose in the sample.

Keywords: azobenzene; high-energy X-ray; isomerization; lipid bilayer; photoswitch; SAXS.

1 Introduction

Azobenzene photoswitches are molecular units, which can be switched between *trans* and *cis* isomer states at the single-molecule level by light. By embedding photoswitches into polymers or supramolecular assemblies containing many individual photoswitch units, materials with mechanical, electrical or optical properties that depend on the *trans/cis* ratio of the photoswitch population can be created: i.e., photoresponsive materials where these properties are adjustable by light [1–6]. Supramolecular assemblies can also provide further degrees of complexity, for example the populations of the two isomers may phase separate [7], or a highly ordered assembly process may select for or stabilise one of the isomer states [8].

As a photoresponsive material's properties depend on the isomer ratio, there is considerable interest in measuring and maximising the degree of switching between mostly-*trans* and mostly-*cis* populations [9]. Typically, it is not possible to perform quantitative photoisomerisations to all-*cis* or to all-*trans* azobenzene populations, due to absorption overlaps [8, 10–13]. Hence, illuminations lead to mixed photostationary state (PSS) populations, with *trans/cis* ratios that depend on the absorption coefficients of the two isomers and the quantum yields of their photoisomerisation. However, a rare example of quantitative switching in one direction (to all-*trans*) was pioneered by Hecht et al. using electrocatalytic pathways that transiently oxidise or reduce the azobenzenes [14–17].

Here we study the switching of photoresponsive lipid membranes assembled from azobenzene-containing

*Corresponding author: Bert Nickel, Faculty of Physics and CeNS, Ludwig-Maximilians-Universität München, Geschwister-Scholl-Platz 1, Munich 80539, Germany, E-mail: nickel@lmu.de. <https://orcid.org/0000-0002-0254-8841>

Martina F. Ober, Anna Baptist and Benjamin Ajanović, Faculty of Physics and CeNS, Ludwig-Maximilians-Universität München, Geschwister-Scholl-Platz 1, Munich 80539, Germany, E-mail: Martina.Ober@physik.lmu.de (M.F. Ober). <https://orcid.org/0000-0001-7827-8027> (M.F. Ober)

Adrian Müller-Deku and Oliver Thorn-Seshold, Department of Pharmacy, Ludwig-Maximilians-Universität München, Butenandtstraße 5-13, Munich 81377, Germany, E-mail: oliver.thorn-seshold@cup.lmu.de (O. Thorn-Seshold). <https://orcid.org/0000-0003-3981-651X> (O. Thorn-Seshold)

Heinz Amenitsch, Institute of Inorganic Chemistry, Graz University of Technology, Stremayrgasse 9, Graz 8010, Austria, E-mail: heinz.amenitsch@elettra.eu. <https://orcid.org/0000-0002-0788-1336>

phosphatidylcholine (azo-PC), a synthetic lipid with a light-responsive azobenzene group in one of its two hydrophobic tails. Optical control of membranes constructed from pure azo-PC allows precise and reversible manipulation of many mechanical properties including membrane shape, permeability, fluidity, and domain formation, and influence membrane protein function [4, 18–21]. So far, it remains unclear how large the changes of *trans/cis* ratio are that cause these property changes; and whether these ratios are close to the theoretical maxima of pure states, or whether they could be substantially improved by tailored conditions and switching stimuli – with associated improvements to switching of biophysical properties [22]. This partly derives from a technical challenge: while it is straightforward to measure *trans/cis* ratios in molecular solutions by a variety of methods, it is not straightforward to measure them in the pure azo-PC membranes. The reason for doubt is that membranes are dense anisotropic assemblies. These give rise to a variety of optical shifts depending on the detailed nature of intermolecular interaction, which are still under investigation [19, 23]. Furthermore, it is widely demonstrated that the azobenzene photoisomerization yield is dramatically improved by embedding amphiphilic azobenzenes in the hydrophobic environment of a lipid membrane [24]. In this study, the synthetic photolipids themselves form the vesicle. Whether the azo-PC membrane's dielectric environment will yield the same protection from the aqueous phase needs to be tested by experiments. For example, ultrastructure studies based on X-ray experiments have shown photostimulated membrane thickness changes of ca. 4 Å for ca. 42 Å azo-PC membranes [4]; but it was not known if this 10% change is already maximal, nor was it known what population-level of *trans/cis* ratios were responsible for this change. Clearly, larger thickness changes would lead to more pronounced biophysically relevant effects.

In this work, we use orthogonal solvent measurements to relate photolipid bilayer thickness to the population-level of *trans/cis* ratios. Comparison of illumination in chloroform and in water reveals an unexpected sensitivity of the photoswitches inside the hydrophobic part of the lipid membrane to the aqueous buffer conditions outside. In water, we observe a smaller-than-expected photoswitching yield under low ionic strength. Furthermore, by mixing pre-switched monomers from chloroform, we show that membrane variations of minimum 8 Å are experimentally possible when photoswitching efficiency is high. In water with high ionic strength, we observe large thickness variations close to illumination in chloroform. These thickness changes are twice as large as thickness variation observed in previous

vesicle photoswitching experiments [4], and much larger than the membrane thickness variations achievable within typical physiologically relevant conditions in natural lipids by change of temperature [25–28].

We also discovered that while hard X-rays do not switch the membranes under study, soft X-rays (8 keV) efficiently and *quantitatively* isomerise photolipid membranes to the all-*trans* state within seconds, which we attribute to radical redox reactions following X-ray dose deposition in the medium. This enables soft X-rays to enforce a higher degree of membrane property control than photoswitching alone can achieve, while emphasising the role of high energy X-rays as low dose probes in soft matter experiments.

2 Materials and methods

2.1 Synthesis of azo-PC and reference photoswitch FAzoM

Azo-PC was purchased from Avanti Polar Lipids, Inc. (Alabama, United States). Novel reference photoswitch FAzoM was synthesised by standard reactions (see Supporting Information).

2.2 Synthesis of azo-PC and reference photoswitches for benchmarking

In our hands, standard techniques to measure *trans/cis* ratios in molecular solutions (H-NMR, HPLC) were not reproducible when applied *in situ* to lipid membranes (ordered assemblies). Destructive readouts (e.g. adding cosolvents to homogenise membrane/water mixtures before HPLC measurement) were also tested but were also not reproducible, which we attributed to difficulties arising from the surfactant nature of the AzoPC. Finally, we developed a method to relate photolipid membrane *trans/cis* isomer ratio to the thickness determined by SAXS by using a calibration series for lipid membranes of known *trans/cis* composition. This series was created by mixing preconditioned all-*trans* and mostly-*cis* stocks (see below). The *trans/cis* ratios in the preconditioned AzoPC stocks were in turn determined by comparison of their UV-Vis spectra with that of the isoelectronic reference photoswitch FAzoM in the same conditions, since the *trans/cis* ratio of the apolar FAzoM can be reliably quantified by HPLC (see Supporting Information section S1 for details).

2.3 Preconditioning and mixing of azo-PC

Azo-PC was dissolved in chloroform (25 mg/mL) and stored at –20 °C until further use. Azo-PC stocks have been stored in dark for several days to reach the all-*trans* state. After illumination of molecularly-dissolved azo-PC by UV-A LED (Roschwege Star-UV365-03-00-00, $\lambda = 365$ nm, 9 nm FWHM, Conrad Electronic SE, Germany) the photostationary state (PSS_{UV}) has a *cis* fraction of 83%

(see Supporting Notes for further detail). To adjust the *cis* fraction in the assembly, we mix azo-PC in the all-*trans* state with azo-PCs with *cis* fraction of 83%, in appropriate proportions. After mixing, we follow the protocol for vesicle preparation. All preparation steps were made in the dark.

2.4 Small unilamellar vesicle (SUV) preparation

The Azo-PC chloroform stock solution was evaporated under a nitrogen stream and stored under vacuum for 12 h. The resulting dry lipid film was dissolved in cyclohexane, and exposed to a vacuum of 6×10^{-3} mbar at a temperature of -60 °C yielding a fluffy lipid powder. Immediately after lyophilisation, the azo-PC powder was hydrated with deionized (DI) water (Milli-Q, Reptile Bioscience Ltd., Boston, MA), or with PBS buffer (pH 7.5), or with 1× TE buffer (10 mM Tris, 1 mM EDTA, pH 8), to a final concentration of 30 mg/mL. The suspension was gently vortexed and subjected to five freeze/thaw cycles. Finally, the sample solution was extruded ca. 25 times through a polycarbonate membrane with a pore diameter of 50–80 nm using a Mini Extruder (Avanti Polar Lipids, Inc., Alabama, United States). The small vesicle size promotes unilamellar membranes [29].

2.5 UV-A/blue light illumination

For photoswitching of azo-PC membranes during SAXS, we built a dual UV-A and blue light LED setup shown in the Supporting Information section S2. For UV-A illumination, we focus a high-power LED (*Roschwege Star-UV365-03-00-00*, $\lambda = 365$ nm, 9 nm FWHM, Conrad Electronic SE, Germany) on the sample capillary. The total maximum optical power of 170 mW and a focal spot size of 4 mm² yield an irradiance of 4.25 W cm⁻². For blue light illumination, fed in by a dichroic mirror, a high-power LED (*Roschwege LSC-B*, $\lambda = 465$ nm, 18 nm FWHM, Conrad Electronic SE, Germany) was used. The blue light is focused with the same focal spot size and a total maximum optical power of 120 mW, resulting in an irradiance of 3.0 W cm⁻². The LEDs and the X-ray detector were remote controlled by TTL signals from an Arduino microprocessor (Reichelt electronics GmbH & Co. KG, Germany). For both LEDs, photostationary states are achieved within a few seconds and multiple switching cycles yield identical SAXS intensities.

2.6 SAXS measurements at 17.4 keV

X-ray data from azo-PC SUVs with preconditioned *trans:cis* ratios were recorded at a Mo-sourced small angle X-ray scattering (SAXS) setup [30]. The Mo anode delivers a beam with an energy of 17.4 keV, a beam size of 1.0 mm², and a flux of $2 \cdot 10^6$ cts·s⁻¹ mm⁻². X-ray data were recorded by a Dectris Pilatus 3R Detector with 487×619 pixels of size 172×172 μm². All in-house SAXS measurements were performed in darkness.

2.7 SAXS measurements at 8 keV

SAXS data from azo-PC SUVs were recorded at the Austrian SAXS beamline at ELETTRA synchrotron using a beam energy of 8 keV [31]

and a beam size of 0.5×2.0 mm². The sample solution was loaded in 1.5–2 mm diameter quartz glass capillaries by flow-through and placed in our UV-A/blue LED setup. A Pilatus detector from Dectris Ltd., Switzerland with 981×1043 pixels of size 172×172 μm² served as detector.

2.8 SAXS measurements at 54 keV

The high energy SAXS data from azo-PC SUVs were recorded at beamline P21.1 at the PETRA III ring at DESY. We measured with a beam energy and size of 54 keV and 1×1 mm², respectively. For the high energy SAXS experiments, the sample solution was first switched optically and then loaded in Kapton tubes of 40 mm in length and 2.5 mm in diameter. A Lambda detector (X-Spectrum GmbH, Germany) with 772×516 pixels with 55×55 μm² pixel size was used.

3 Results and discussion

Azo-PC monomers dissolved in low-dielectric chloroform are driven towards *cis*-rich photostationary state by UV-A light at 365 nm, and towards *trans*-rich state by blue light of 465 nm (Figure 1a). The absorption spectra of these mixed states, either in molecular solution or in assemblies, have been reported by us and others [4, 18, 19] and substantial differences between them have been noted [19]. Previously, we have used SAXS to determine the membrane thickness for blue or UV light photostationary states reached in lipid vesicles in DI water [4]. Here, we prepared calibration series of azo-PC vesicles of known *trans/cis* ratios by mixing stocks of dark-adapted all-*trans* azo-PC with 83% *cis* azo-PC (see methods and SI). We use calibrants of 0%, 10%, 19%, 39%, 58% and 83% *cis* isomers to cover the full range of ratios accessible during membrane photoswitching, with an estimated error margin of $\pm 5\%$ of the given value to account for mixing precision as well as *cis* fraction uncertainties in the preconditioned samples. The referencing method developed to determine the stock *cis* percentage is novel in this field. This method can prove generally useful for analysis of systems which lack reliable bulk references, i.e. which cannot be interpreted with help of UV-Vis spectra of monomer solution, see Methods and Supporting Information for details.

The SAXS measurements for these calibrant ratios are summarized in Figure 1b. The X-ray intensity distributions are typical for lipid bilayer samples [32, 33] and are stable over several hours (see Figure S3). The distributions vary strongly with the *trans*-to-*cis* ratio, e.g. the intensity dip around $q = 0.05$ Å⁻¹ shifts consecutively to higher q -values with increasing *cis* content. This indicates that the membrane thickness decreases with increasing *cis* isomer fraction. To extract the head-to-head distances d_{HH} , we model the SAXS intensities in Figure 1b by an established lipid

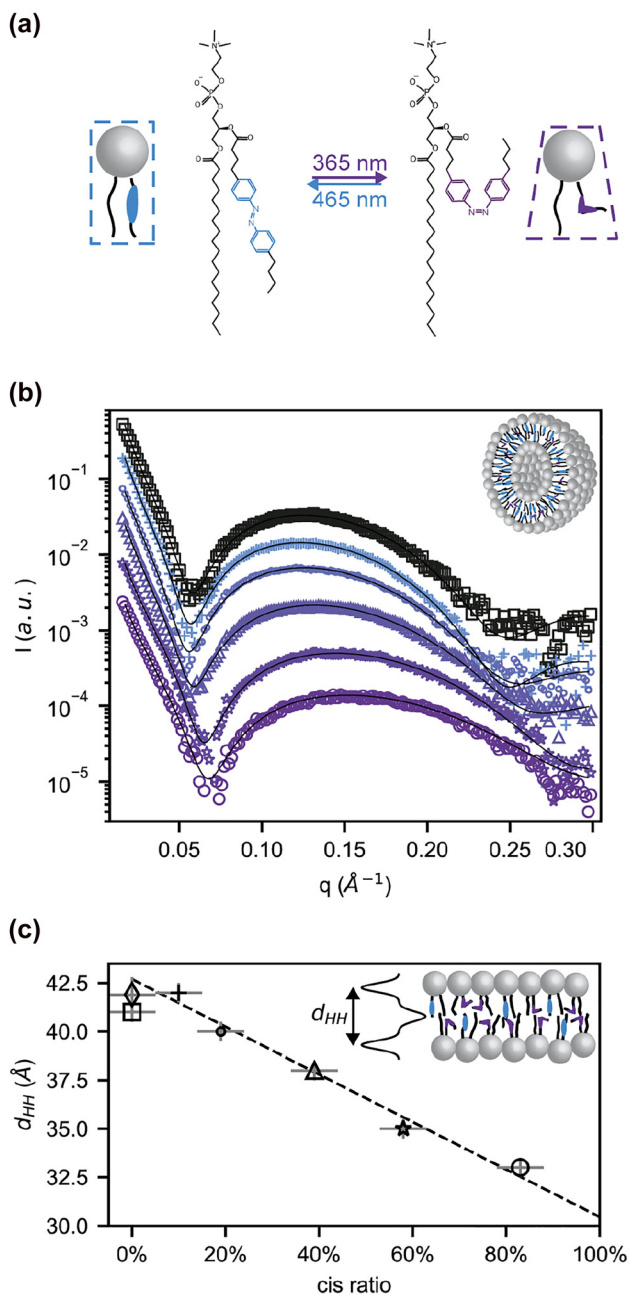


Figure 1: X-ray structural data of photoswitchable membranes. (a) Schematic representation of the chemical structure of the azo-PC photolipids used in this study and their *trans* and *cis* configuration. (b) SAXS intensities for unilamellar azo-PC vesicles prepared from predefined *trans* to *cis* ratios: Dark-adapted state (100:0), (90:10), (81:19), (61:39), (42:58) and (17:83) are shown as squares, crosses, dots, triangles, stars, and circles. Intensities are vertically offset for clarity. (c) Head-to-head distance (d_{HH}) of azo-PC membranes as function of the percentage of azo-PCs in *cis* isomerization state are shown with the same symbols as in (b). Additionally, the mean value of d_{HH} for the dark-adapted photostationary states obtained from azo-PC SUVs in DI water (Figure 2b) is shown as diamond. The linear fit of d_{HH} in dependence of *cis* isomer percentage is indicated as dashed line. See Supporting Information (section S8) for details.

bilayer electron density profile, using the software SasView (see Supporting Information section S6) [34]. The results of this analysis are shown in Figure 1c. The dark-adapted state shows a head-to-head-distance of d_{HH} ($0 \pm 5\%$ *cis*) = $40.9 \pm 0.6 \text{ \AA}$. The analysis reveals that the thickness of the azo-PC membrane depends almost linearly on the *trans*-to-*cis* ratio over a broad range. Increasing the percentage of *cis* azo-PC thins the membrane down to d_{HH} ($83 \pm 5\%$ *cis*) = $33.0 \pm 0.5 \text{ \AA}$ for 83% *cis*. Thus, the membrane thickness changes by 8 \AA .

In the following measurements, we use this relation between membrane thickness and *cis* fraction to infer the *cis* fraction of various photostationary states in response to illumination and buffer conditions (Figure 1). Our previous photoswitching experiments have been performed on vesicles in deionized water (DI water): a common choice for lipids since DI water facilitates unilamellar membrane formation by increasing lipid vesicle stability. The maximal membrane thickness change obtained by optical switching under these conditions was only 4 to 5 \AA . The new experiments with premixed lipids reported in Figure 1 now reveal that this optical control window covers only about half of the thickness change effect which could be achieved in ideal photoswitching conditions. We therefore studied two widely used buffer systems, phosphate-buffered saline

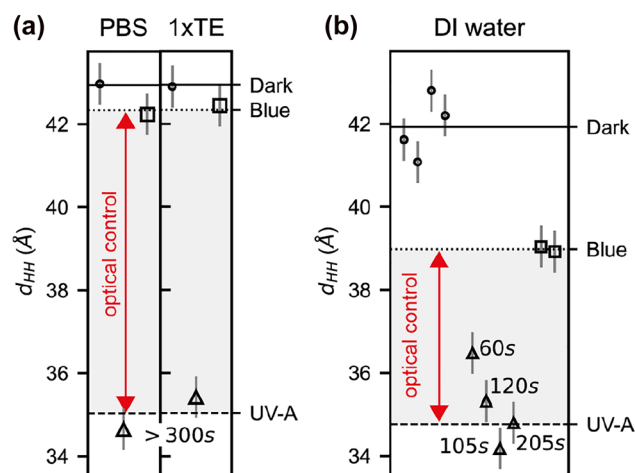


Figure 2: Switching behaviour of photomembranes in buffer and in DI water.

(a) Head-to-head distances (d_{HH}) obtained for azo-PC SUVs in PBS and 1xTE buffer. (b) d_{HH} obtained for azo-PC SUVs in DI water. The dark-adapted state, and several photostationary states induced via UV-A and blue light are labelled accordingly. Horizontal lines indicate mean values of d_{HH} for the dark-adapted, UV-A, and blue light photostationary states, shown as solid, dashed, and dotted line, respectively. The exposure time of UV-A light while approaching the photostationary state is indicated in seconds. The optical control window for the different buffer conditions is indicated by a red double-headed arrow.

(PBS), and a mixture of Tris with EDTA (1×TE), for their influence on the optical control window. The analysis of the SAXS data is condensed in Figure 2, the full data set is shown in Figures S4 and S5a.

The dark-adapted states (all-*trans*) yielded mean membrane thicknesses of d_{HH} (dark, buffers) = $42.9 \pm 0.2 \text{ \AA}$ and d_{HH} (dark, deionized water) = $41.9 \pm 0.9 \text{ \AA}$ (Figure 2a and b, circles, solid line). Hence, all conditions allow for the formation of dense, all-*trans* membranes in the dark. To photoswitch towards high *cis* contents, UV-A illumination was used until a photostationary state was achieved. Independent of the usage of buffer or not, the UV photostationary states do not reach a *cis* fraction of 83% as obtained by preconditioning monomers in chloroform. Instead, the observed membrane thicknesses of $d_{\text{HH}}^{\text{UV}} = 34.8 \pm 0.6 \text{ \AA}$ (see Figure 2b, dashed line and Figure S5) indicates *cis* contents around 64%. This is not unexpected, given the blue-shifting of azobenzene absorption spectra seen upon going from molecular solutions to assembled systems [19].

However, when using blue light to photoswitch from a *cis*- to a *trans*-enriched state, the outcomes depend greatly on whether the system is buffered or not. In DI water, the maximal blue light photostationary state membrane thickness is $d_{\text{HH}}^{\text{blue}} = 39.0 \pm 0.3 \text{ \AA}$ (Figure 2b, squares, dotted line), i.e. 30% *cis* isomer still remains. Instead, in PBS or 1× TE buffer, the membrane thickness increases to $d_{\text{HH}}^{\text{blue}} = 42.3 \pm 0.4 \text{ \AA}$ (Figure 2a, squares, dotted line), i.e. only 3% *cis* isomer remains. Optical control of vesicles is therefore highly efficient in these buffered aqueous solutions. Follow up experiments with NaCl solutions (see Figure S9), indicate that ionic strength rather than pH buffering is key to efficient photoswitching towards *trans*-enriched states in lipid vesicles. This effect is not observed for molecular monomers in aqueous solutions, where azobenzenes lose their ability to efficiently isomerize anyway [24]. Increasing ionic strength was reported to remove water molecules from inside the membrane promoting tighter packing of lipids [35, 36]. This should enhance the protection of the azobenzene photoswitch from water.

Next, we explored possible influence of X-ray on photostationary states. For this study, we used X-ray exposures to deposit a certain X-ray dose into the vesicle solution, i.e. a certain energy of absorbed X-rays per mass of the exposed sample [37]. The X-ray absorption drops drastically for increasing energies and in turn high X-ray energies enable low-dose SAXS experiments and vice versa (cf. Figure S7 and Note S7). Thus, the dosing experiment was conducted as follows. First, we prepared the vesicles in a high *cis* fraction by UV-A illumination. Next, we exposed the sample to a rather high X-ray energy of 54 keV for 60 s.

Five such consecutive exposures yield an identical SAXS signal. There is no sign of any hard X-ray induced effects after 5 min in total, even though this experiment was performed at a high brilliance Petra III synchrotron beamline with full beam on the sample, cf. Figure 3a. This finding is in agreement with the fact that the cross section for photoabsorption is dramatically reduced for high X-ray energies.

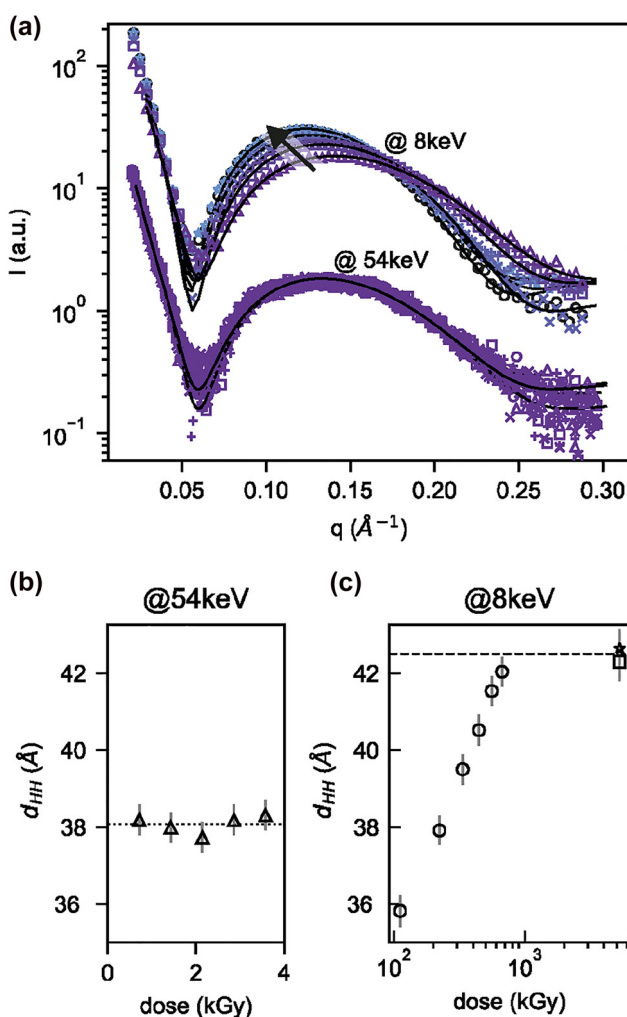


Figure 3: Catalytic switching of photomembranes induced by soft X-rays.

(a) After initial UV illumination, two different X-ray SAXS experiments are performed at 8 and 54 keV on unilamellar photolipid vesicles. Solid curves indicate modelling of the SAXS data by symmetrical bilayers. (b) Head-to-head distances (d_{HH}) obtained for azo-PC SUVs in DI water as function of X-ray dose measured at 54 keV. Dotted line indicates the mean value of d_{HH} for the stable UV-A induced PSS. (c) d_{HH} obtained for azo-PC SUVs in DI water as function of X-ray dose measured at 8 keV. Horizontal dashed line indicate the average d_{HH} after saturating 8 keV X-ray exposure.

Depositing high doses in water requires soft X-rays (discussion in the Supporting Information section S7). Such soft X-rays give rise to radiolysis of water, and oxidising and reducing radicals and reactive species [38, 39], which may provide pathways for catalytic redox-based unidirectional switching towards the thermodynamic groundstate (all-*trans*) [15]. Therefore, we tested also the change of membrane thickness during six consecutive 8 keV X-ray exposures each of 2 s (Figure 3a). After each X-ray exposure, a shift of the SAXS pattern was visible. To quantify the thickness change of the photomembrane, we modelled to extract the head-to-head distances, which increased dramatically after each soft X-ray exposure, depending on the total delivered X-ray dose. Remarkably, the final mean membrane thickness of $d_{\text{HH}}^{\text{xray}} = 42.5 \pm 0.3 \text{ \AA}$ (Figure 3b, star and square datapoints at high dose, dashed line; Figure S5b) matches the thickness of the dark-adapted all-*trans* state $d_{\text{HH}}^{\text{dark}} = 41.9 \pm 0.9 \text{ \AA}$ (Figure 2b, circular data points from repeated measurements, solid line). This is a direct indication of quantitative switching obtained by 8 keV X-ray exposure.

These X-ray induced changes of the isomerisation state of the azobenzene photoswitch are fully reversible and should not be mistaken as irreversible radiation damage. They can however be employed as a reversible X-ray dose readout. To demonstrate this, we plot the membrane thickness as observed by hard X-ray SAXS in response to soft X-ray exposure with dose expressed in kGray [kGy] in Figure 3b. The calculation of the dose, a routine calculation in radiation protection, is explained in the Supporting Information. Here, quantitative switching starts above 100 kGy, and saturates for an X-ray dose above 700 kGy. We propose that the measurement of azo-PC *cis* to *trans* transition for SUVs in DI water can be used to read out the effective X-ray dose in a regime of up to 700 kGy. This range may help to calibrate critical doses for biological SAXS experiments which can range from 51 kGy [40], to 400 kGy [41], to 284–7056 kGy [38].

The SAXS signal is almost independent of the X-ray energy (Figure S7, inset). Therefore, the minimum of the X-ray dose for samples with high water fraction at 36 keV (Figure S7) should be used to prevent radiation effects. Our experiments demonstrate that high quality SAXS data may be obtained even for weakly scattering biological samples.

4 Conclusions and summary

SAXS with hard X-rays provides a direct read out of the membrane bilayer thickness. We find that membrane thickness has a linear dependency of photolipid

isomerization fraction. The 8 Å thickness change accessible by photoswitching in buffered solutions (20% of the membrane thickness) is massive, and apparently only possible because the membrane itself seals the azobenzene from the unfavourable polar solvent. Hydrophobic matching of membrane thickness with trans-membrane proteins is a wide research field that could benefit enormously from the large thickness change effects observed here [42]. Due to the rapid development of high power UV-A LEDs, and the availability of pulsed UV-A lasers at synchrotron sources [43], we expect that future experiments with pulsed illumination may allow rapid membrane thickness transition times of few ms and below. At these short timescales, the hydrodynamic coupling of the intercalated water to the photolipids may give rise to further interesting transient phenomena [25]. We also highlight the versatility of high energy X-rays as low-dose probes.

Acknowledgements: This work benefited from SasView software, originally developed by the DANSE project under NSF award DMR-0520547. The authors acknowledge the CERIC-ERIC Consortium for the access to experimental facilities. Portions of this research were carried out at the light source PETRA III at DESY, a member of the Helmholtz Association (HGF). We would like to thank Oleh Ivashko for assistance in using beamline P21.1 for high energy experiments.

Author contribution: MFO performed vesicle preparation, and SAXS experiments and X-ray data analysis, and wrote the manuscript; AMD performed synthesis of azo-PC and FAzoM, and spectroscopic and HPLC analyses of *cis/trans* isomer ratios; AB developed a protocol for photolipid SUV preparation; BA performed the SAXS experiments in NaCl solution; HA enabled the SAXS experiments at ELETTRA and provided in depth expertise on SAXS calibration and data conversion; OTS designed *cis/trans* ratio measurements and wrote the manuscript; BN designed the study, and joined the X-ray experiments, and wrote the manuscript.

Research funding: We acknowledge financial support by the German Research Foundation (DFG) through SFB1032 (Nanoagents) projects A07 (to B.N.) and B09 (to O.T.-S.) number 201269156, SFB TRR 152 project P24 number 239283807 to O.T.-S., Emmy Noether grant TH2231/1-1 to O.T.-S., and SPP 1926 project number 426018126 to O.T.-S.; by the Federal Ministry of Education and Research in Germany (BMBF) grant no. 05K19WMA (LUCENT) to B.N.; and by the Bavarian State Ministry of Science, Research, and Arts grant “SolarTechnologies go Hybrid (SolTech)” to B.N.

Conflict of interest statement: The authors declare no conflicts of interest regarding this article.

References

- [1] Y. Yu, M. Nakano, and T. Ikeda, "Directed bending of a polymer film by light," *Nature*, vol. 425, no. 6954, p. 145, 2003.
- [2] M. Hoshino, E. Uchida, Y. Norikane, et al., "Crystal melting by light: X-ray crystal structure analysis of an azo crystal showing photoinduced crystal-melt transition," *J. Am. Chem. Soc.*, vol. 136, no. 25, pp. 9158–9164, 2014.
- [3] F. Reise, J. E. Warias, K. Chatterjee, et al., "Photoswitchable glycolipid mimetics: synthesis and photochromic properties of glycoazobenzene amphiphiles," *Chem. Eur J.*, vol. 24, no. 66, pp. 17497–17505, 2018.
- [4] P. Urban, S. D. Pritzl, M. F. Ober, et al., "A lipid photoswitch controls fluidity in supported bilayer membranes," *Langmuir*, vol. 36, no. 10, pp. 2629–2634, 2020.
- [5] A. Goulet-Hanssens, F. Eisenreich, and S. Hecht, "Enlightening materials with photoswitches," *Adv. Mater.*, vol. 32, no. 20, p. 1905966, 2020.
- [6] D.-Y. Kim, T. Christoff-Tempesta, G. Lamour, X. Zuo, K.-H. Ryu, and J. H. Ortony, "Morphological transitions of a photoswitchable aramid amphiphile nanostructure," *Nano Lett.*, vol. 21, no. 7, pp. 2912–2918, 2021.
- [7] R. H. Zha, G. Vantomme, J. A. Berrocal, et al., "Photoswitchable nanomaterials based on hierarchically organized Siloxane Oligomers," *Adv. Funct. Mater.*, vol. 28, no. 1, p. 1703952, 2018.
- [8] Z. Wu, R. Xue, M. Xie, et al., "Self-assembly-triggered cis-to-trans conversion of azobenzene compounds," *J. Phys. Chem. Lett.*, vol. 9, no. 1, pp. 163–169, 2018.
- [9] F. A. Jerca, V. V. Jerca, and R. Hoogenboom, "Advances and opportunities in the exciting world of azobenzenes," *Nat. Rev. Chem.*, vol. 6, pp. 51–69, 2021.
- [10] Y. Lin, X. Cheng, Y. Qiao, et al., "Creation of photo-modulated multi-state and multi-scale molecular assemblies via binary-state molecular switch," *Soft Matter*, vol. 6, no. 5, pp. 902–908, 2010.
- [11] D. Bléger, J. Schwarz, A. M. Brouwer, and S. Hecht, "o-Fluoroazobenzenes as readily synthesized photoswitches offering nearly quantitative two-way isomerization with visible light," *J. Am. Chem. Soc.*, vol. 134, no. 51, pp. 20597–20600, 2012.
- [12] C. Weber, T. Liebig, M. Gensler, et al., "Cooperative switching in nanofibers of azobenzene oligomers," *Sci. Rep.*, vol. 6, no. 1, p. 25605, 2016.
- [13] M. Baroncini, J. Groppi, S. Corra, S. Silvi, and A. Credi, "Light-responsive (supra)molecular architectures: recent advances," *Adv. Opt. Mater.*, vol. 7, no. 16, p. 1900392, 2019.
- [14] A. Goulet-Hanssens, M. Utecht, D. Mutruc, et al., "Electrocatalytic Z → E isomerization of azobenzenes," *J. Am. Chem. Soc.*, vol. 139, no. 1, pp. 335–341, 2017.
- [15] A. Goulet-Hanssens, C. Rietze, E. Titov, et al., "Hole catalysis as a general mechanism for efficient and wavelength-independent Z → E Azobenzene Isomerization," *Inside Chem.*, vol. 4, no. 7, pp. 1740–1755, 2018.
- [16] J. L. Greenfield, M. A. Gerkman, R. S. L. Gibson, G. G. D. Han, and M. J. Fuchter, "Efficient electrocatalytic switching of azoheteroarenes in the condensed phases," *J. Am. Chem. Soc.*, vol. 143, no. 37, pp. 15250–15257, 2021.
- [17] K. Kuntze, J. Isokuortti, A. Siiskonen, N. Durandin, T. Laaksonen, and A. Priimagi, "Azobenzene photoswitching with near-infrared light mediated by molecular oxygen," *J. Phys. Chem. B*, vol. 125, no. 45, pp. 12568–12573, 2021.
- [18] C. Pernpeintner, J. A. Frank, P. Urban, et al., "Light-controlled membrane mechanics and shape transitions of photoswitchable lipid vesicles," *Langmuir*, vol. 33, no. 16, pp. 4083–4089, 2017.
- [19] P. Urban, S. D. Pritzl, D. B. Konrad, et al., "Light-controlled lipid interaction and membrane organization in photolipid bilayer vesicles," *Langmuir*, vol. 34, no. 44, pp. 13368–13374, 2018.
- [20] S. D. Pritzl, P. Urban, A. Prasselsperger, et al., "Photolipid bilayer permeability is controlled by transient pore formation," *Langmuir*, vol. 36, no. 45, pp. 13509–13515, 2020.
- [21] M. Doroudgar, J. Morstein, J. Becker-Baldus, D. Trauner, and C. Glaubitz, "How photoswitchable lipids affect the order and dynamics of lipid bilayers and embedded proteins," *J. Am. Chem. Soc.*, vol. 143, no. 25, pp. 9515–9528, 2021.
- [22] J. Pfeffermann, B. Eicher, D. Boytsov, et al., "Photoswitching of model ion channels in lipid bilayers," *J. Photochem. Photobiol. B Biol.*, vol. 224, p. 112320, 2021.
- [23] S. D. Pritzl, D. B. Konrad, M. F. Ober, et al., "Optical membrane control with red light enabled by red-shifted photolipids," *Langmuir*, vol. 38, no. 1, pp. 385–393, 2021.
- [24] G. M. Paternò, E. Colombo, V. Vurro, et al., "Membrane environment enables ultrafast isomerization of amphiphilic azobenzene," *Adv. Sci.*, vol. 7, no. 8, p. 1903241, 2020.
- [25] G. Pabst, M. Rappolt, H. Amenitsch, S. Bernstorff, and P. Laggner, "X-ray kinematography of temperature-jump relaxation probes the elastic properties of fluid bilayers," *Langmuir*, vol. 16, no. 23, pp. 8994–9001, 2000.
- [26] M. Rappolt, F. Vidal, M. Kriechbaum, et al., "Structural, dynamic and mechanical properties of POPC at low cholesterol concentration studied in pressure/temperature space," *Eur. Biophys. J.*, vol. 31, no. 8, pp. 575–585, 2002.
- [27] S. Leekumjorn and A. K. Sum, "Molecular characterization of gel and liquid-crystalline structures of fully hydrated POPC and POPE bilayers," *J. Phys. Chem. B*, vol. 111, no. 21, pp. 6026–6033, 2007.
- [28] N. Kucerka, M.-P. Nieh, and J. Katsaras, "Fluid phase lipid areas and bilayer thicknesses of commonly used phosphatidylcholines as a function of temperature," *Biochim. Biophys. Acta Biomembr.*, vol. 1808, no. 11, pp. 2761–2771, 2011.
- [29] H. L. Scott, A. Skinkle, E. G. Kelley, M. N. Waxham, I. Levental, and F. A. Heberle, "On the mechanism of bilayer separation by extrusion, or why your LUVs are not really unilamellar," *Biophys. J.*, vol. 117, no. 8, pp. 1381–1386, 2019.
- [30] L. K. Bruetzel, S. Fischer, A. Salditt, S. M. Sedlak, B. Nickel, and J. Lipfert, "A Mo-anode-based in-house source for small-angle X-ray scattering measurements of biological macromolecules," *Rev. Sci. Instrum.*, vol. 87, no. 2, 2016, Art no. 025103.
- [31] H. Amenitsch, S. Bernstorff, and P. Laggner, "High-flux beamline for small-angle X-ray scattering at ELETTRA," *Rev. Sci. Instrum.*, vol. 66, no. 2, pp. 1624–1626, 1995.
- [32] M. R. Brzustowicz and A. T. Brunger, "X-ray scattering from unilamellar lipid vesicles," *J. Appl. Crystallogr.*, vol. 38, no. 1, pp. 126–131, 2005.
- [33] K. Komorowski, A. Salditt, Y. Xu, et al., "Vesicle adhesion and fusion studied by small-angle X-ray scattering," *Biophys. J.*, vol. 114, no. 8, pp. 1908–1920, 2018.
- [34] M. Doucet, J. H. Cho, G. Alina, et al., *SasView version 4.2, Zenodo 2018*, <https://doi.org/10.5281/zenodo.1412041>.

- [35] S. Šegota, D. Vojta, G. Pletikapić, and G. Baranović, “Ionic strength and composition govern the elasticity of biological membranes. A study of model DMPC bilayers by force- and transmission IR spectroscopy,” *Chem. Phys. Lipids*, vol. 186, pp. 17–29, 2015.
- [36] P. Mukhopadhyay, L. Monticelli, and D. P. Tieleman, “Molecular dynamics simulation of a palmitoyl-oleoyl phosphatidylserine bilayer with Na⁺ counterions and NaCl,” *Biophys. J.*, vol. 86, no. 3, pp. 1601–1609, 2004.
- [37] F. H. Attix, *Introduction to Radiological Physics and Radiation Dosimetry*, Weinheim, Wiley VCH, 2004.
- [38] C. M. Jeffries, M. A. Graewert, D. I. Svergun, and C. E. Blanchet, “Limiting radiation damage for high-brilliance biological solution scattering: practical experience at the EMBL P12 beamline PETRAIII,” *J. Synchrotron Radiat.*, vol. 22, no. 2, pp. 273–279, 2015.
- [39] J. L. Dickerson and E. F. Garman, “The potential benefits of using higher X-ray energies for macromolecular crystallography,” *J. Synchrotron Radiat.*, vol. 26, no. 4, pp. 922–930, 2019.
- [40] J. C. Brooks-Bartlett, R. A. Batters, C. S. Bury, et al., “Development of tools to automate quantitative analysis of radiation damage in SAXS experiments,” *J. Synchrotron Radiat.*, vol. 24, no. 1, pp. 63–72, 2017.
- [41] S. Kuwamoto, S. Akiyama, and T. Fujisawa, “Radiation damage to a protein solution, detected by synchrotron X-ray small-angle scattering: dose-related considerations and suppression by cryoprotectants,” *J. Synchrotron Radiat.*, vol. 11, no. 6, pp. 462–468, 2004.
- [42] T. M. Weiss, P. C. A. van der Wel, J. A. Killian, R. E. Koeppe, and H. W. Huang, “Hydrophobic mismatch between helices and lipid bilayers,” *Biophys. J.*, vol. 84, no. 1, pp. 379–385, 2003.
- [43] M. Burian, B. Marmiroli, A. Radeticchio, et al., “Picosecond pump-probe X-ray scattering at the Elettra SAXS beamline,” *J. Synchrotron Radiat.*, vol. 27, no. 1, pp. 51–59, 2020.

Supplementary Material: The online version of this article offers supplementary material (<https://doi.org/10.1515/nanoph-2022-0053>).